

# Direct observation by resonant tunneling of the $B^+$ level in a delta-doped silicon barrier

J. Caro, I.D. Vink, G.D.J. Smit, S. Rogge, and T.M. Klapwijk

*Department of NanoScience, Delft University of Technology, Lorentzweg 1, 2628 CJ Delft, The Netherlands*

R. Loo and M. Caymax

*IMEC, Kapeldreef 75, B-3001 Leuven, Belgium*

(Dated: 11th November 2018)

We observe a resonance in the conductance of silicon tunneling devices with a  $\delta$ -doped barrier. The position of the resonance indicates that it arises from tunneling through the  $B^+$  state of the boron atoms of the  $\delta$ -layer. Since the emitter Fermi level in our devices is a field-independent reference energy, we are able to directly observe the diamagnetic shift of the  $B^+$  level. This is contrary to the situation in magneto-optical spectroscopy, where the shift is absorbed in the measured ionization energy.

The smallest semiconductor device with potential functionality is a semiconducting nanostructure with a single dopant atom. The properties of such a structure are most prominent at low temperature, where the electron or hole is localized at the parent donor or acceptor, respectively. Manipulation of the wave function of the charge carrier at the dopant atom with the electric field of a gate is the obvious tool to influence the properties of the nanostructure. A good first order description of the properties of dopant atoms is given by the hydrogen model<sup>1</sup>. The resulting Bohr radius of up to about 10 nm sets the size of a dopant atom and thus of a single-dopant-atom functional device. This radius is much larger than for the hydrogen atom, due to scaling for the effective mass of the carrier and the dielectric constant of the semiconductor. Such dimensions are accessible with e-beam lithography and scanning probe techniques. This opens the way for what can be called atomic scale electronics inside a semiconductor. Silicon is very attractive for this purpose because of its highly developed fabrication technology.

A beautiful example of atomic scale electronics inside silicon is the quantum computer proposed by Kane<sup>2</sup> and by Skinner *et al.*<sup>3</sup>. Both the fabrication and electrical operation of the qubits of this computer rely on control at the level of individual phosphorus donors. The highly controlled dopant engineering required for atomic scale electronics inside silicon is being worked on by several groups<sup>4,5</sup>. Doping at the atomic scale for application purposes is thought to be feasible, but development of this technique will be time consuming.

A more direct way to a single dopant atom in silicon, albeit less controlled concerning exact positioning, is to use  $\delta$ -doping and conventional nanostructuring. Single-dopant-atom structures fabricated in this way will yield physics relevant for future devices fabricated with atomic scale doping techniques. To some extent this approach has been followed already, by including a  $\delta$ -layer of dopant atoms in the well of double barrier diodes<sup>6</sup>. Here, we report a transport study on  $\delta$ -doped silicon tunneling devices grown with a single barrier. The dopant atoms induce zero-dimensional atomic quantum wells, giving

many identical double barrier systems in parallel. This device, a precursor of a single-dopant-atom device of a geometry close to a qubit of Kane's computer, shows very interesting transport properties. In particular, we find a conductance resonance due to tunneling through the boron impurities of the  $\delta$ -layer in the barrier. The position of the resonance and its magnetic field dependence indicate that it originates from tunneling through the  $B^+$  state of the boron impurities. So far, this state has only been observed in spectroscopic studies using photons or phonons and not in an energy resolved transport experiment like ours.

We fabricate the  $\delta$ -doped devices from a layered structure of the type  $p^+ \text{Si}(500 \text{ nm})/p^- \text{Si}(20 \text{ nm})/\delta/p^- \text{Si}(20 \text{ nm})/p^+ \text{Si}(500 \text{ nm})$ . Boron is the dopant, for the layers and the  $\delta$ -spike. The structure is deposited by chemical vapor deposition in an ASM Epsilon 2000 reactor on a Si(001) substrate with low doping, using  $\text{SiH}_4$  and  $\text{B}_2\text{H}_6$  as precursor gasses. The  $\delta$ -spike of areal density  $1.7 \times 10^{11} \text{ cm}^{-2}$  is centered in the lowly doped 40 nm thick tunnel barrier. The  $p^+$  layers are degenerately doped ( $N_B = 10^{19} \text{ cm}^{-3}$ ) and serve as contact layers. The devices are square mesas, 100, 200, 300 and 400  $\mu\text{m}$  at a side. They are dry-etched in an  $\text{SF}_6$  plasma. The etch mask is the Al-1%Si top contact of the mesa, which is sputter-deposited through a shadow mask. The  $\text{SF}_6$  etch is stopped just after the bottom  $p^+$  layer has been reached. A second shadow mask, aligned with respect to the mesas, is used for sputter deposition of Al-1%Si contacts to the bottom layer. The final step is a 400 °C anneal in  $\text{N}_2/\text{H}_2$  of the Al contacts to the  $p^+$  Si, using rapid thermal processing. A high device quality is apparent from resistance scaling with mesa size. At room temperature the resistance is dominated by the two-dimensional spreading resistance of the bottom layer between the mesa and the Al contact, while at low temperature it is determined by the barrier in the mesa. These devices, which have a metal-insulator-metal structure, are the simplest all-silicon tunneling devices.

We measured the doping profile in the structure with secondary ion mass spectroscopy (SIMS). Figure 1(a)

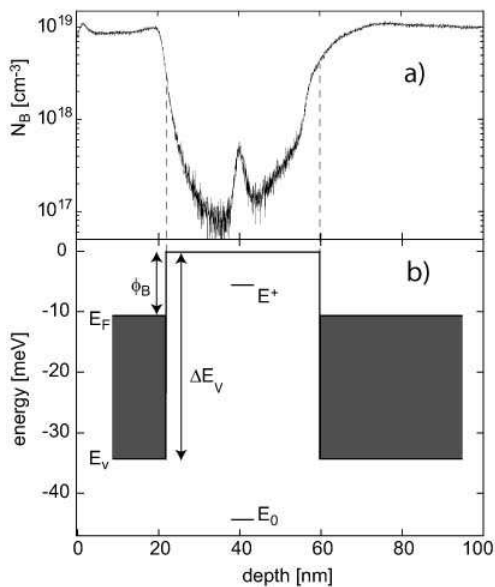


Figure 1: (a) SIMS profile of the boron concentration. Zero depth is the surface position. For optimum resolution the top layer is only 20 nm thick. Contact layers, barrier and  $\delta$ -layer are clearly visible. (b) Depicts the profile of the valence-band edge, the hole energy increasing in the upward direction. Fermi seas of emitter and collector extend up to the barrier, of which the thickness is defined with the criterion  $N_B = 4 \times 10^{18} \text{ cm}^{-3}$ , the concentration of the metal-insulator transition. Symbols are discussed in the text.

gives the result, in which the  $\delta$ -layer, the barrier and the contact layers are clearly discernible. The  $\delta$ -layer is about 6 nm wide and has a peak concentration of  $N_B = 5 \times 10^{17} \text{ cm}^{-3}$ . The contrast of the  $\delta$ -layer and the background doping ( $N_B \approx 10^{17} \text{ cm}^{-3}$ ) in the barrier is somewhat weak, although for the barrier  $\text{B}_2\text{H}_6$  is only applied during  $\delta$ -doping. This is due to boron diffusion during the silicon growth, out of the  $\text{p}^+$  bottom layer and out of the  $\delta$ -layer. The profile of the valence band edge is depicted in Fig. 1(b). The tunnel-barrier height is<sup>7</sup>  $\phi_B = \Delta E_v - E_F$ , *i.e.* the valence-band contribution  $\Delta E_v$  to the band-gap narrowing of emitter and collector minus the Fermi energy  $E_F$  of these device layers.

Electrical measurements were performed in a flow cryostat equipped with a 14 T superconducting magnet and in a  $^3\text{He}$  cryostat. We use standard lock-in techniques to measure  $G - V$  curves, *i.e.* curves of the differential conductance versus bias. In the  $G - V$  curves, at 4.2 K and below, a tunneling resonance is present around 10 mV, superimposed on a dominant background. In Fig. 2 we show curves of a 400  $\mu\text{m}$  device, for temperatures between 0.5 and 12.5 K. The weak resonance at 4.2 K becomes a clear peak at lower temperature, which is not yet saturated at 0.5 K. At this temperature the FWHM of the peak is about 1.5 mV. The overall behavior as sketched in Fig. 2 is present for all measured devices, which are of different size and come from different fabri-

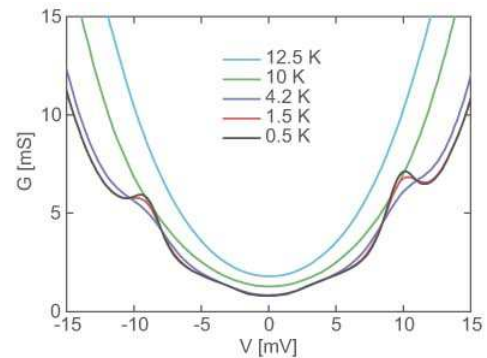


Figure 2: Conductance curves of 400  $\mu\text{m}$  device 1/888/1, for the temperatures listed. With decreasing temperature the conductance decreases (for the lower temperatures most clear at higher biases) and a resonance at  $\pm 10$  mV develops. Between 1.5 and 0.5 K the resonance still grows.

cation runs. The peak is absent for devices that have no  $\delta$ -layer but are otherwise identical. This indicates that the peak originates from the boron atoms of the  $\delta$ -layer.

In the inset of Fig. 3 we plot the response of the spectra (background subtracted) to a magnetic field, for the same device as in Fig. 2, for one bias polarity<sup>8</sup> and for fields up to 14 T oriented perpendicular to the layers. With increasing field the peak shifts to higher bias and becomes broader and lower. In the main panel of Fig. 3 data points of the level shift  $\Delta E = \frac{1}{2}e\Delta V_{\text{res}}$  deduced from the resonance shift  $\Delta V_{\text{res}}$  (see below for the relation between level and resonance positions) follow a weak quadratic function of the field, the shift at 14 T being about 1 mV. This behavior does not depend on the orientation of the field with respect to the crystallographic axes of the device.

The conductance peak is attributed to resonant tunneling through the  $\text{B}^+$  state of boron impurities in the  $\delta$ -layer, each of which provides for a conductance channel. The  $\text{B}^+$  state is an acceptor counterpart of the more generally known  $\text{D}^-$  state<sup>9</sup>. It forms when a second hole is weakly bound to a neutral acceptor, in our case neutral boron  $\text{B}^0$ . In zero magnetic field the  $\text{B}^+$  state is a singlet state (as the  $\text{D}^-$  state is), which is analogous to the negative hydrogen ion<sup>9</sup> ( $\text{H}^-$  ion). The separation of the  $\text{B}^0$  ground-state level and the  $\text{B}^+$  level results from the Coulomb interaction between the holes. In our devices the  $\text{B}^0$  ground state is deep below the Fermi level, so that it is permanently occupied. Therefore, higher levels of the  $\text{B}^0$  single hole spectrum are not available as stepping stones for holes tunneling from emitter to collector. This means that the  $\text{B}^+$  state is the only candidate which can induce the resonance. This is unlike an optical absorption experiment in which higher levels may always come into play via transitions from the ground state<sup>1</sup>.

From photoconductance spectroscopy on Si samples with low doping level it is known<sup>10</sup> that in zero magnetic field the binding energy  $E^+(0)$  of the extra hole on an isolated  $\text{B}^+$  ion, *i.e.* the amount of energy required to

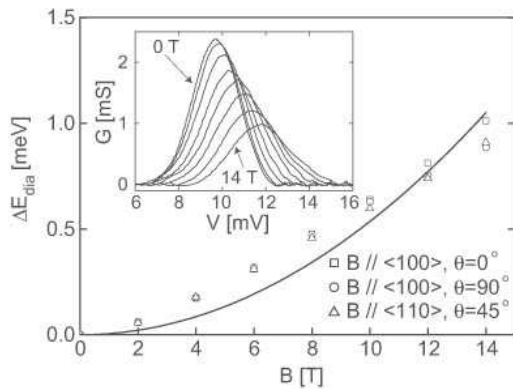


Figure 3: Magnetic field induced shift of the discrete energy level in the barrier of device 1/888/1, for three field orientations and for three angles  $\theta$  between field and current direction. The parabola is a fit of the expression for the diamagnetic shift of the  $B^+$  level to the data points. The data points are derived from curves as in the inset, which shows the field dependence of the resonance of device 1/888/1 (the field step is 2 T).

remove this hole from the ion to the valence band edge, is about 2.0 meV. This is close to  $0.055\text{Ry}^* = 2.5$  meV predicted by the  $H^-$  ion model, which is successfully used for the  $D^-$  state<sup>9</sup>. Here  $\text{Ry}^*$  is the effective Rydberg for boron in silicon, which equals the ground state energy  $E_1 = 45.7$  meV<sup>1</sup>. Since the measured resonance comes from the  $\delta$ -layer, equal parts of the bias drop across the barriers at either side of the Coulombic potential well associated with a boron impurity. Thus, the resonance voltage is  $V_{\text{res}} = 2[\phi_B - E^+(0)]/e$  [see Fig. 1(b)]. We determine  $\phi_B$  from the temperature dependence of the zero-bias resistance  $R_0$ . When plotted versus  $1/T$ , the logarithm  $\ln(T^2 R_0)$  clearly shows activated behaviour in the range 15-20 K. Interpreting this as Richardson-Dushman thermionic emission<sup>11</sup> of holes over the barrier, we find  $\phi_B = 11.7$  meV from a fit to the data. This is not too far from  $\phi_B = \Delta E_v - E_F = 8$  meV, which we obtain from the estimate<sup>12</sup> for  $\Delta E_v(N_B)$  and from photoluminescence measurements<sup>13</sup> of  $E_F(N_B)$ , each subject to uncertainty. The values  $\phi_B = 11.7$  meV and  $E^+(0) = 2.0$  meV predict  $V_{\text{res}} = 19.4$  mV. This deviates strongly from the measured position and thus seems to exclude the  $B^+$  state. However, the concentration  $N_B = 5 \times 10^{17} \text{ cm}^{-3}$  of the  $\delta$ -layer is high enough for the tail of the wave function of the second hole to be appreciable at the nearest  $B^0$  atoms<sup>14</sup>, so that the  $B^+$  ions are not isolated. The additional Coulomb attraction of these  $B^0$  atoms and spreading of the electron charge among them (reducing the hole-hole repulsion at the  $B^+$  state) cause a stronger binding. This effect increases with increasing concentration. The measured  $V_{\text{res}} \approx 10$  mV gives  $E^+(0) \approx 6.7$  meV. As demonstrated in Fig. 4, this value nicely falls in the bandwidth obtained by extrapolating the scarce experimental data<sup>14,15,16</sup> on the concentration dependence of the ionization energy for  $B^+$  and  $D^-$ .

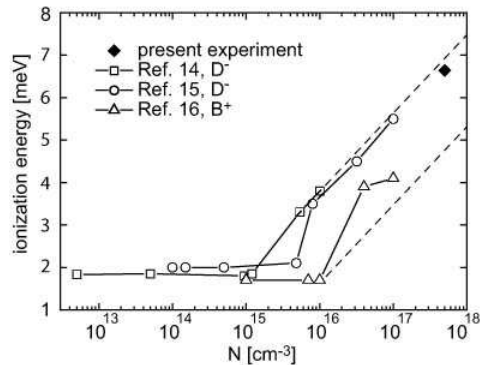


Figure 4: Plot of experimental ionization energies for  $B^+$  and  $D^-$  versus doping concentration (from literature). Above  $N \approx 10^{15} \text{ cm}^{-3}$  the ionization energy increases. The data point of the present work ( $\blacklozenge$ ) nicely falls in the extrapolated bandwidth which indicates the trend of the literature data.

In the lower part of the temperature range of Fig. 2 the resonance is much wider than the theoretical width  $3.5kT$  of a Fermi-smearred sharp resonance, implying a rather large zero temperature width ( $\approx 1.5$  meV). Mechanisms contributing to this are life-time broadening, disorder broadening and broadening due to the finite width of the  $\delta$ -layer. Life-time broadening determines the intrinsic width of a resonance coming from a single impurity. For the  $B^+$  level life-time broadening is appreciable, since it is so close to the ionization level. The effect is enhanced by the large bias field at resonance (2.5 kV/cm), which weakens the collector barrier and thus shortens the life time. We will come back to this in discussing broadening of the resonance with increasing magnetic field (see below). Disorder broadening arises from the different local surrounding of  $B^0$  centers by adjacent  $B^0$  centers, which causes a distribution of levels. The finite width of the  $\delta$ -layer implies a range of values of  $V_{\text{res}}$ , since the position of the atom defines the barrier thicknesses and thus the distribution of the bias over them. Without correcting for a decay of the resonance for off-center positions<sup>17</sup>, a range for  $V_{\text{res}}$  of 3.5 mV is derived from only the finite  $\delta$ -layer width. We take this as a sign that the  $\delta$ -layer width is an important source of broadening.

The resonance shift to higher bias (Fig. 3) reflects the diamagnetic shift  $\Delta E_{\text{dia}}(B)$  of the  $B^+$  level in a magnetic field. This shift, termed diamagnetic because of the related negative susceptibility, is towards the valence band edge, in agreement with the observed peak shift to higher biases. In magneto-optical spectroscopy the diamagnetic shift is not obtained directly, since it is absorbed in the field-dependent binding energy  $E^+(B) = E^+(0) + \frac{1}{2}\hbar\omega - \Delta E_{\text{dia}}(B)$ . Here  $\frac{1}{2}\hbar\omega$  is the energy of the first Landau level, which is the valence-band edge in field. In our experiment, however, since the emitter doping level  $N_B = 10^{19} \text{ cm}^{-3}$  is high enough to block Landau level formation in this layer, the emitter Fermi level is a field-independent reference energy enabling direct mea-

surement of  $\Delta E_{\text{dia}}(B)$ . For the weak fields used here, first order perturbation theory estimates the diamagnetic shift as<sup>18</sup>  $\Delta E_{\text{dia}}(B) = \frac{e^2 B^2}{12m} \sum_i \overline{r_i^2}$ . Here  $m$  is the effective mass of the holes of the  $B^+$  ion and  $\overline{r_i^2}$  is the mean square distance of the  $i$ -th hole to the  $B^-$  core ( $i = 1, 2$ ). Taking<sup>19</sup>  $m_{lh} = 0.15m_0$  and  $m_{hh} = 0.54m_0$  for the light and heavy hole masses, respectively, and  $\overline{r_1^2} = a_0^2$  for the first hole ( $a_0 = 3.9$  nm is the Bohr radius of the  $B^0$  atom), we fit the expression for  $\Delta E_{\text{dia}}(B)$  to the complete set of data points of Fig. 3. This yields the fit shown in the figure and corresponding values  $\overline{r_2^2} = (1.6a_0)^2$  and  $\overline{r_2^2} = (3.4a_0)^2$ . The range defined by these values is consistent with  $r_2 = 2.4a_0$  cited for the  $B^+$  state<sup>20</sup>. We attribute the deviation of the fitted curve from the experimental trend to the use of an atomic physics model for  $\Delta E_{\text{dia}}$  in a solid state system.

Broadening of the resonance with increasing magnetic field may be unresolved splitting and/or life-time broadening induced by the Stark effect. Since the resonance voltage increases with increasing magnetic field, the electric field at resonance, and thus the Stark broadening, increase as well. Data for Stark broadening of the  $B^+$  level are not available. Therefore, we take as a measure the broadening of the far infrared absorption line due to transition from the ground state of  $B^0$  atom in silicon to the first excited state, which was measured up to 1.0 kV/cm<sup>21</sup>. Extrapolation of the data of Ref. [21] to the fields of our experiments yields an increase of the halfwidth between 0 T and 14 T of 0.1 meV, to be compared with our measured increase of 0.5 meV. Stark broadening apparently plays a role.

Finally, we discuss the background contribution to the conductance (see Fig. 2), which shows a weak temperature dependence below 4.2 K. The parabolic shape of the background suggests direct tunneling as transport mechanism. However, the conductance at  $V = 0$  is several orders of magnitude higher than expected for direct tun-

neling<sup>22</sup>, so that it is excluded. Hence, the background conductance is due to hopping resulting from the background doping in the barrier. This hopping is thermally activated close to  $V = 0$  and field activated at higher biases ( $|V| \geq 2$  mV). For biases exceeding the barrier height ( $|V| \geq 11.7$  mV), the barrier becomes increasingly weak for hopping and finally for direct tunneling, giving a further conductance increase. Above 4.2 K the conductance in the range ( $|V| \leq 2$  mV) undergoes a transition to coexistence of thermal hopping and thermal activation over the barrier and finally to dominance of activation over the barrier.

In conclusion, we have studied resonant tunneling through a Si barrier  $\delta$ -doped with boron impurities. The conductance resonance observed is due to tunneling through the  $B^+$  state of the impurities. The structure of our device enables direct observation of the diamagnetic shift of the  $B^+$  state. The measured magnitude of the shift agrees well with the theoretical description, yielding a proper value of the orbit size for the second hole of the  $B^+$  state. The binding energy of the  $B^+$  state turns out to be enhanced as a result of overlap of the wave function of the second hole of the  $B^+$  state with the nearest boron impurities. Our next step will be miniaturizing the devices to the level of one dopant atom (diameter  $\approx 50$  nm), enabling studies of the effect of wave-function manipulation on transport through the atom.

We acknowledge valuable discussions with G.E.W. Bauer, T.O. Klaassen and J.R. Tucker. M. van Putten is acknowledged for his contributions in the initial phase of the work. This work is part of the research program of the Stichting voor Fundamenteel Onderzoek der Materie, which is financially supported by the Nederlandse Organisatie voor Wetenschappelijk Onderzoek. One of us, S.R., wishes to acknowledge the Royal Netherlands Academy of Arts and Sciences for financial support.

- 
- <sup>1</sup> A.K. Ramdas and S. Rodriguez, Rep. Prog. Phys. **44**, 1336 (1981).  
<sup>2</sup> B.E. Kane, Nature **393**, 133 (1998).  
<sup>3</sup> A.J. Skinner, M.E. Davenport and B.E Kane, Phys. Rev. Lett. **90**, 87901 (2003).  
<sup>4</sup> J.R. Tucker and T.C. Shen, Solid-State Electronics **42**, 1061 (1998).  
<sup>5</sup> T. Schenkel *et al.*, J. Vac. Sci. Technol. B **20**, 2819 (2002).  
<sup>6</sup> J.G.S. Lok *et al.*, Phys. Rev. B **53**, 9554 (1996), and references therein.  
<sup>7</sup> H.X. Yuan and A.G.U. Perera, J. Appl. Phys. **79**, 4418 (1996).  
<sup>8</sup> The conductance curves are very symmetric, so that it suffices to measure for only one bias polarity.  
<sup>9</sup> D.M. Larsen, Phys. Rev. Lett. **42**, 742 (1979).  
<sup>10</sup> V.N. Aleksandrov, E.M. Gerschenzon, A.P. Mel'nikov, R.I. Rabinovich, N.A. Serebryakova, JETP Lett. **22**, 282 (1975).  
<sup>11</sup> K.C. Kao and W. Hwang, *Electrical Transport in Solids, International Series in the Science of the Solid State, Volume 14* (Pergamon Press, Oxford, 1981).  
<sup>12</sup> S.C. Jain and D.J. Roulston, Solid-State Electronics **34**, 453 (1991).  
<sup>13</sup> W.P. Dumke, J. Appl. Phys. **54**, 3200 (1983).  
<sup>14</sup> P. Norton, Phys. Rev. Lett. **37**, 164 (1976).  
<sup>15</sup> M. Taniguchi and S. Narita, Sol. State Comm. **20**, 131 (1976).  
<sup>16</sup> W. Burger and K. Lassmann, Phys. Rev. B **33**, 5868 (1986).  
<sup>17</sup> V. Kalmeyer and R.B. Laughlin, Phys. Rev. B **35**, 9805 (1987).  
<sup>18</sup> L.D. Landau and E.M. Lifshitz, *Quantum Mechanics (non-relativistic theory), Course of Theoretical Physics, Volume 3* (Butterworth-Heinemann, Oxford, 2000), third edition.  
<sup>19</sup> Both light and heavy holes tunnel, so that an average hole mass applies here. However, non-parabolicity and warpage

of the bands and uncertainty in the Fermi energy make the masses uncertain. Therefore, we prefer to estimate a range of Bohr radii from the limiting mass values, which are taken from H.D. Barber, *Solid-State Electronics* **10**, 1039 (1967).

<sup>20</sup> E.M. Gershenzon, Yu.A. Gurvich, A.P. Mel'nikov, L.N.

Shestakov, *Sov. Phys. Semicond.* **25**, 95 (1991).

<sup>21</sup> J.J. White, *Can. J. Phys.* **45**, 2695 (1967).

<sup>22</sup> This follows from the expression for the tunneling conductance. See for example R. Meservey and P.M. Tedrow, *J. Appl. Phys.* **53**, 1563 (1982).